AD-A130 310 A COMPARISON OF THE STRENGTHS OF METAL-METAL AND METAL-CFRP (CARBON FIBRE..(U) ROYAL AIRCRAFT ESTABLISHMENT FARNBOROUGH (ENGLAND) M H STONE OCT 82 RAE-TR-82102 DRIC-BR-87429 1/1

UNCLASSIFIED F/G 11/6 NL

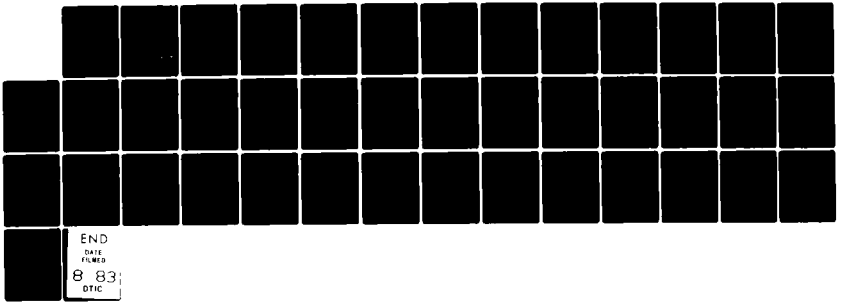

END

DATE FILMED

8 83

DTIC

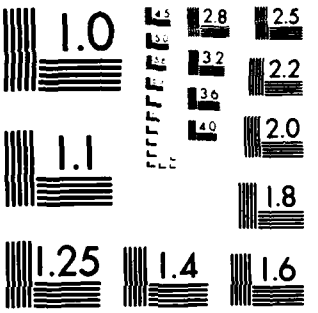

TR 82102

ROYAL AIRCRAFT ESTABLISHMENT

*

Technical Report 82102

October 1982

A COMPARISON OF THE STRENGTHS OF METAL-METAL AND METAL-CFRP ADHESIVE BONDED JOINTS AT VARIOUS TEST TEMPERATURES

by

M. H. Stone

*

Procurement Executive, Ministry of Defence
Farnborough, Hants

UDC 621.792.052 : 621.792.3 : 621.792.4 : 539.4

ROYAL AIRCRAFT ESTABLISHMENT

Technical Report 82102

Received for printing 27 October 1982

A COMPARISON OF THE STRENGTHS OF METAL-METAL AND METAL-CFRP ADHESIVE BONDED JOINTS AT VARIOUS TEST TEMPERATURES

by

M. H. Stone

SUMMARY

Tests on double lap joints bonded with a range of adhesives showed that differential thermal contraction of the adherends in metal-CFRP joints can greatly reduce strengths relative to metal-metal joints, particularly at low temperatures. However, the effect varied widely between adhesives, and relatively high strengths were obtained for an adhesive with a high strain to failure.

Strengths of metal-CFRP joints were much higher when titanium was substituted for aluminium, as expected from the lower expansion coefficient of titanium. However, attempts to reduce thermal stress by lowering the stress-free temperature with the use of reduced cure temperatures were unsuccessful, possibly because the adhesives did not develop their full toughness.

The low transverse tensile strength of CFRP also contributed in some cases to the reduced strength of metal-CFRP joints, relative to metal-metal joints.

(Selected data from this work were reported at the PRI Conference Adhesion and Adhesives, Durham, September 1980, and published as M.H. Stone, Int. J. Adhesion and Adhesives, 1, 203-207 (1981) and ibid., 1, 271-272 (1981).)

Departmental Reference: Materials/Structures 13

LIST OF CONTENTS

		Page
1	INTRODUCTION	3
2	THEORY	3
	2.1 List of symbols	3
	2.2 Shear stresses at the ends of the overlap	4
	2.3 Role of peel stresses in causing failure of metal-CFRP joints	5
3	EXPERIMENTAL METHODS	6
	3.1 Materials	6
	3.2 Surface pretreatment and priming of adherends	7
	3.3 Manufacture and testing of joints	7
4	RESULTS	8
	4.1 Heat distortion temperatures of adhesives	8
	4.2 Joint strengths and modes of failure	8
5	DISCUSSION	9
	5.1 Heat distortion temperatures of adhesives	9
	5.2 Joint strengths	9
	5.2.1 Metal-metal joints	9
	5.2.2 Metal-CFRP joints	10
	5.2.3 Effect of adhesive mechanical properties on the strength of metal-CFRP joints	11
6	CONCLUSIONS	12
Appendix A	Stresses in the adhesive	13
Appendix B	Processing and properties of CFRP laminates	17
Appendix C	Surface pretreatment and priming of adherends	19
Tables 1 to 5		23
References		28
Illustrations		Figures 1-9
Report documentation page		inside back cover

1 INTRODUCTION

The durability of metal-metal adhesive joints in warm humid conditions is a potential problem in aerospace structures[1,2], although recent improvements in primers, adhesives and metal surface pretreatments now permit much longer lives[3,4]. However, the use of carbon fibre reinforced plastics (CFRP) bonded to metals adds two new threats to durability, namely differential thermal contraction of adherends and increased risk of corrosion due to galvanic action[5,6]. Differential contraction from the cure temperature produces an inherent stress in the joint, which will reduce the joint strength, particularly at low temperatures. Both this stress and the increased corrosion risk could reduce durability.

The work described concerns only the thermal stress effect, which was assessed by comparing metal-CFRP joints with metal-metal joints. Only initial strengths are reported here, measured at -55°C, room temperature (RT) and +80°C for a range of adhesives. Modified cure cycles are examined, and comparison is made between aluminium and titanium adherends for one adhesive. Results are discussed in terms of differential contraction, peel stresses in the joints, and the stress-strain characteristics of the adhesives. Durability studies are in progress and will be reported separately, the present Report being the first of a series.

2 THEORY

2.1 List of symbols (refer to Fig 1)

b = width of joint (m)

d = thickness of adhesive layer (m)

E = Young's modulus of adherend (Pa)

E'_A = constrained Young's modulus of adhesive (Pa)

G = shear modulus of adhesive (Pa)

$K = \sqrt{\frac{2G}{d(Et)}}$ (m^{-1})

$K' = \sqrt{\frac{G}{d}\left(\frac{1}{E_1 t_1} + \frac{1}{E_2 t_2}\right)}$ (m^{-1})

ℓ = overlap length (m)

P = half the external load on the joint (N)

t = adherend thickness (m)

T_d = heat distortion temperature of adhesive (°C)

ΔT = working temperature - stress-free temperature (K)

x = longitudinal coordinate (m)

α = coefficient of linear thermal expansion (K^{-1})

$\Delta\alpha = \alpha_2 - \alpha_1$ (K^{-1})

ν_2 = Poisson's ratio of adherend 2

σ = peel stress normal to the plane of the joint at $x = 0$ (Pa)

τ = shear stress in the adhesive (Pa)

Subscripts

1,2 refer to adherends 1, 2

T indicates shear stress due only to thermal mismatch

L indicates shear stress due only to applied load

max indicates shear stress at ends of overlap

2.2 Shear stresses at the ends of the overlap

The magnitude of the thermal stresses and the effects of varying parameters may be estimated by shear lag analysis assuming linear elastic behaviour of the adhesive[7] (see Appendix A, section A.2, for details). For the symmetrical balanced double lap joint shown in Figs 1 to 3, in which dimensions are chosen so that $E_1t_1 \simeq E_2t_2 = (Et)$, the peak shear stresses in the adhesive at the ends of the overlap, due to thermal mismatch alone, are equal and opposite in sign and given approximately by

$$T\tau_{max} = \pm \Delta\alpha\Delta T\sqrt{\frac{G(Et)}{2d}} \quad . \tag{1}$$

The corresponding peak shear stresses due to an external load $2P$ alone are also equal, but of the same sign at both ends, and are given by

$$L\tau_{max} = \frac{P}{2b}\sqrt{\frac{2G}{d(Et)}} \quad . \tag{2}$$

(Note that for the materials and joint geometry used in the present work the peak shear stress is almost independent of overlap length for ℓ greater than ~10 mm.)

The CFRP-metal joints (Fig 3) consisted of central adherends (No.1) of CFRP and outer adherends (No.2) of metal. The peak shear stresses due to external load and thermal mismatch at low temperature were therefore additive at the ends of the outer adherends with this arrangement and load direction, and this is also where the stress normal to the plane of the joint is tensile. This form of joint therefore presents a 'worst case'. The stresses are simply additive, so the following expression gives the approximate total peak shear stress in the adhesive at the ends of the outer metal adherends,

$$\tau_{max} = L\tau_{max} + T\tau_{max} \simeq \frac{P}{2b}\sqrt{\frac{2G}{d(Et)}} - \Delta\alpha\Delta T\sqrt{\frac{G(Et)}{2d}} \quad . \tag{3}$$

(Note that for most service conditions ΔT is negative.)

The most influential parameters for thermal stress are $\Delta\alpha$ and ΔT, and both were varied in the present work. Values of α for metals and various forms of CFRP are shown in Table 1; $\Delta\alpha$ ranges from 1 to 22 $\times 10^{-6}$ K^{-1} depending on the metal-CFRP combination. In this work unidirectional CFRP was used in conjunction with either aluminium or titanium alloys, giving an almost 3-fold difference in $\Delta\alpha$, with the aluminium-CFRP joint representing the worst case.

Attempts were also made to investigate the effect of reducing ΔT, whose value in practice is the difference between operating and stress-free temperatures of the joint. The minimum operating temperature for aircraft structures is defined by the ambient temperature at high altitudes, usually taken as $-55^{\circ}C$, thus ΔT can only be reduced by lowering the stress-free temperature. The latter is either: (a) the adhesive cure temperature if this is lower than its heat distortion temperature T_d, or, (b) T_d if this is lower than cure temperature. (Cooling from cure temperature to T_d introduces only small stresses because the adhesive modulus is low above T_d.) Upper operating temperature requirements limit the scope for reducing T_d, which must exceed the service

temperature by a margin sufficient to avoid excessive creep during prolonged load. In the present case the adhesives are regarded as capable of operation at 80°C and thus a minimum T_d of 90°C was chosen, with T_d preferably no higher than 100°C in order to keep ΔT to a minimum. Thus to achieve a major reduction in ΔT adhesives should be curable at temperatures well below the necessary minimum T_d (*ie* case (a) above) but such ideal materials do not seem to be available. In this work modest reductions in ΔT were however achieved by reducing cure temperature, or by selecting adhesives with T_d in the range 90-100°C. In particular, an attempt was made to reduce the stress-free temperature by using room-temperature curing adhesives which were post-cured in stages at successively higher temperatures to achieve the desired T_d .

The importance of thermal stress is exemplified by the following estimates for aluminium alloy-CFRP joints bonded with a typical 120°C-curing toughened epoxy adhesive (see Appendix A for full details).

(a) Joint at -55°C with no external load and $\Delta T = -150$ K; from equation (1) ${}_T\tau_{max} = 72.1$ MPa .

(b) Joint at 10°C with applied load of 15% of strength and $\Delta T = -85$ K (this is typical of joints now undergoing outdoor exposure at RAE):

from equation (2) ${}_L\tau_{max} = 11.6$ MPa;
from equation (1) ${}_T\tau_{max} = 40.9$ MPa;
therefore $\tau_{max} = 52.5$ MPa.

The ${}_T\tau_{max}$ values are clearly overestimates because they lie above the linear elastic region for which the analysis is valid; and in example (a) the value of ${}_T\tau_{max}$ exceeds the strength of most adhesives. Nevertheless, the preponderance of thermal stress is *striking*.

2.3 Role of peel stresses in causing failure of metal-CFRP joints (see Appendix A, section A.3 for details)

Using the approximate analysis of Hart-Smith[8], peel stress at the ends of the outer *adherends (x = 0 in Fig 1) is given by*

$$\sigma = \tau \left[\frac{3E'_A (1 - \nu_2^2) t_2}{E_2 d} \right]^{\frac{1}{4}} . \qquad (4)$$

E'_A is the constrained tensile modulus of the adhesive, which will be considerably higher than Young's modulus as usually measured. Of the materials used in the present work data are available only for adhesive B for which E'_A is about 9 GPa[9], while the maximum plastic shear stress τ is 45 MPa [10]. Thus, from equation (4) maximum values of σ were calculated as 72.4 MPa for aluminium alloy outer adherends and 57.5 MPa for titanium alloy outer adherends. Both values are much higher than the composite transverse tensile strength (TTS) of 39.4 MPa (Table B1). With increasing load failure is therefore expected to occur within the composite as τ reaches a value at which $\sigma = 39.4$ MPa, provided the adhesive tensile strength is greater than this. It should be

noted that, in contrast to the TTS, composite shear strength is 81.9 MPa, much higher than adhesive shear strength.

3 EXPERIMENTAL METHODS

3.1 Materials

(a) Alloys. Clad aluminium alloy sheet was to BS L73, 2 mm thick for outer adherends, and 4 mm thick for the central adherend of metal-metal joints (Figs 2 and 3). Titanium alloy 6Al4V sheet was to BS TA10, 1.2 mm thick for outer adherends and 2 mm thick for the central adherend of metal-metal joints.

These alloys are widely used in aerospace structures and are the subject of continuing durability studies of metal-metal joints[1,2,4].

(b) CFRP. The carbon fibre was type 140SC/10000 at nominally 60% volume fraction in matrix resin Shell DX210 with DX137 hardener. The unidirectional layup was autoclave cured 2 h at 120°C with PTFE-coated glass cloth as release sheets, to give boards nominally 2 mm thick (*ie* t_1 = 1 mm). Interlaminar shear strength (ILSS) was 81.9 MPa, transverse tensile strength (TTS) was 39.4 MPa, and void content was 1.35%.

Details of the CFRP are given in Appendix B.

(c) Adhesives. These were all toughened materials intended for aerospace structural use, chosen from a wide selection after trials[11].

Adhesive B. This is described as a modified epoxy (probably a nitrile-epoxy), and is a film supported on a Dacron random mat; the recommended cure is 1 h at 120°C. It was used with Primer 1, described as a modified epoxy-phenolic. This is a curing primer that contains chromate for corrosion inhibition.

Adhesive C. This film is described as a modified epoxy (again, probably a nitrile-epoxy), supported on a knitted nylon cloth; recommended cure is 0.5 h at 120°C. It was used with Primer 2, described as a modified epoxy resin solution, which is believed to contain chromate; this was also a curing primer.

Adhesive E. This is a one-part paste adhesive described as a modified epoxy; recommended cure is 1 h at 120°C. It was used with Primer 1.

Adhesive M3. This is a two-part amine-hardened epoxy paste adhesive that cures to a brittle gel at room temperature and requires elevated temperature post-cure to develop strength and toughness. Actual cures used are shown in Table 2. It was used with Primer 2.

Adhesive R1. This is a two-part acrylate with a peroxide catalyst that gives a room temperature cure. However, it was additionally post-cured as shown in Table 2 to give the desired T_d. It was used with Primer 1.

Adhesive M3 contained glass ballotini to give a lower limit of glue line thickness of 0.1 mm. Similar ballotini were added to E and R1 at a concentration of 1.5% by weight. The ballotini had been treated with appropriate silane coupling-agents to improve bonding to the resin.

3.2 Surface pretreatment and priming of adherends (for full details see Appendix C)

Aluminium alloy plates were first cleaned by solvent swabbing, vapour degreasing, and immersion in a proprietary alkaline solution. Bonding pretreatment then consisted of chromic-sulphuric acid pickling followed by phosphoric acid anodising. Titanium alloy plates were solvent swabbed, wet blasted with 180 grade alumina grit, and etched in alkaline peroxide solution[4]. CFRP was solvent swabbed, dry blasted with 280 grade alumina grit and finally brush swabbed with 2-butanone to remove grit and debris. The grit blasting was lightly done to avoid exposing carbon fibres. Primers were sprayed on to give a coating thickness of about 2-3 μm.

3.3 Manufacture and testing of joints

Joints were bonded as panels; the metal adherends had been preslotted before surface treatment so that individual joints could be separated without having to cut through a metal/CFRP sandwich, which would have caused excessive heating. The adherend plates had also been machined with locating slots and holes at the ends of the overlap region, which fitted over pins on a baseplate to give the required overlap. This arrangement also allowed for differential thermal expansion of adherends and baseplate.

The two-part adhesives were mixed by kneading them in polythene bags from which the air had been expelled. This prevented incorporation of air bubbles which could lead to voidy joints and reduced loss of volatile monomer from adhesive R1. In addition it protected the amine-cured epoxy from possible effects of atmospheric CO_2 and H_2O, and the acrylate from the inhibiting effects of oxygen. (During cure of the acrylate adhesive it was necessary to bathe the joint panels in N_2 to prevent cure inhibition, which otherwise affected a band 1-2 mm wide around the edge of the bond area.)

Cure was carried out at 180 kPa pressure, using an autoclave for adhesives B and C, and a press for E, M3 and R1, according to the alternative cure or post-cure cycles for each adhesive shown in Table 2. In the autoclave the layup was evacuated and left overnight under vacuum. Pressure was then applied and the vacuum released before starting the cure cycle; heat-up rates were about 2 K/min in both autoclave and press. Some of the post-cures for adhesives M3 and R1 were done in an oven.

Joints were essentially the same form as used in the continuing series of outdoor exposure trials tnat have been in progress since 1967 [1]. They were nominally 25 mm wide by 12.5 mm overlap (Figs 2 and 3) and were cut from the bonded panels, using a band saw on the metal adherends and a diamond-tipped slitting wheel for the CFRP. Glue line thickness for adhesive C ranged from 0.10 to 0.19 mm with most values close to 0.15 mm; for the other adhesives the range was 0.04 to 0.18 mm with most values close to 0.10 mm. Thicknesses were more variable for metal-CFRP joints because of local variations in the CFRP thickness. Completed joints were stored sealed in polythene bags containing silica gel.

Breaking loads were measured on six replicates at a crosshead speed of 1 mm/min, and strengths were calculated from the actual measured dimensions of the lap area in which failure occurred. It was normally possible to determine which side of the joint failed because the other outer adherend was left with a sharp bend at the end of the overlap caused by the eccentric load path that was momentarily sustained; where this was

not clear the mean of the two lap areas was used for calculating strength. When testing at -55°C and +80°C the joints were kept at these temperatures for 10 min before applying load. Proportions of the various failure modes were assessed visually, and where necessary supplemented by microscope examination. Joints with obvious faults, such as large voids, were excluded from calculation of the mean.

4 RESULTS

4.1 Heat distortion temperatures of adhesives

Interpretation of the joint strength results is aided by data on T_d for the adhesives: Table 2 gives values determined for the products and cures used in the present work[11,12]. T_d lay in the range 95-120°C for all the adhesives with most values close to 100°C, adhesive E being the exception.

4.2 Joint strengths and modes of failure

Joint strengths at +80°C, RT and -55°C and coefficients of variation are shown in Table 3 for metal-CFRP joints and the analogous metal-metal joints for each adhesive with alternative cures. Adhesive C was used with both aluminium and titanium alloy outer adherends to show the effect of reducing $\Delta\alpha$. The effect of thermal mismatch stress is shown in the final column of Table 3, where the metal-CFRP strength is expressed as a percentage of the metal-metal strength. Failure modes are summarised in Tables 4 and 5, abbreviated as follows:

AC = adhesion to composite;

AM = adhesion to metal;

CA = cohesive within the adhesive + primer layer, including failure at the primer/adhesive interface;

CC = cohesive within the composite. This mode of failure was always close to the composite surface, in some areas leaving only the surface skin of matrix resin attached to the metal adherend, in other areas leaving a thin layer of carbon fibres as well. There was no correlation of strength with the relative proportion of these two sub-modes.

The metal-metal joints failed mainly cohesively (CA), although much of this failure was close to the surface, usually of the central adherend and particularly for joints tested at -55°C. It was often difficult to locate the failure path within the layer of primer + adhesive: failure may have occurred at the primer/adhesive interface, within the primer layer, or within the adhesive close to the primer. There were no obvious correlations between failure modes and joint strengths.

Predominant failure modes for the metal-CFRP joints varied with adhesive and test temperature. Failure was mainly in the composite for adhesives C and E, and for B tested at -55°C, whereas B failed mainly in the adhesive when tested at RT or +80°C. Adhesive R1 showed a high proportion of CA failure close to the surface of the central adherend, as was observed for the corresponding metal-metal joints. The contrast in failure modes between B and R1, which used the same primer, is assumed to reflect their differing mechanical properties: there is some evidence that R1 is more brittle at low

temperature. With the exceptions discussed below there were no clear correlations between joint strengths and modes of failure. Also, there was no evidence that voids in the CFRP were a cause of failure (see Appendix B, section B.4).

Adhesive M3 behaved anomalously in giving very high scatter and unexpectedly low mean strengths in metal-CFRP joints, in contrast to values obtained in preliminary trials and for metal-metal joints, so additional joints were tested at RT (Table 3). A clear correlation emerged between low strength and a high proportion of AC failure, which in turn was related to incomplete abrasion of the CFRP surface (Figs 4 to 6)[13,14].

5 DISCUSSION

5.1 Heat distortion temperatures of adhesives

Extended cure times at 90°C for epoxy adhesives B, C and E gave values of T_d which were almost as high as those given by conventional cures at 120°C (Table 2): for adhesive E a 30 K reduction in ΔT was thus achieved by curing at 90°C. Also, preliminary measurements of strengths of aluminium-aluminium single lap joints bonded with five epoxy adhesives including B and C showed values for the 90°C cure mainly within ±10% of those obtained with the normal 120°C cure[11]. Alternative cure temperatures of 90°C and 120°C were therefore used in the present work for the hot curing epoxy adhesives to assess the effect of reducing ΔT on the strength of metal-CFRP joints.

Both of the two-part, cold setting adhesives R1 and M3 required post-curing at elevated temperatures. Adhesive R1 cured only at RT gave a temperature-deflection trace that indicated rapid further curing during measurement, but prior post-curing eliminated this effect[11]; adhesive M3 was brittle and weak after a RT cure and was designed to be post-cured. For both adhesives an attempt was therefore made to reduce the stress-free temperature, and hence reduce ΔT, by using multi-stage post-cures at successively increasing temperature levels, as detailed in Table 2; these multi-stage cures were compared with single-stage post-cures. For the multi-stage post-cures it was postulated that cross-links formed in the lower temperature stages would not completely re-arrange or relax during subsequent higher temperature cure stages. The stress-free temperature of these original cross-links would therefore remain below the final cure temperature; and they would serve to lower the overall average stress-free temperature observed for the final cross-linked network as a whole. Thus it was expected that the multi-stage post-cures would give lower stress-free temperatures than the single-stage post-cures, even though final cure temperatures were the same and the alternative cures gave the same T_d values (Table 2).

5.2 Joint strengths

5.2.1 Metal-metal joints

Strengths of the metal-metal joints (Table 3) were typical of modern toughened structural adhesives and compare well with the manufacturers' values, although the low values for adhesive R1 at -55°C suggest brittleness at this temperature. Reduced cure temperature was satisfactory with adhesive C, but B was substantially weaker at -55°C and E was weaker at both RT and -55°C, perhaps because the physical structure required for

toughness was not properly developed in a 90°C cure. For adhesive M3 the multi-stage post-cure gave the same strength at RT as the single-stage post-cure but substantially weaker joints at -55°C. For adhesive R1 the alternative cures also gave similar strengths at RT but in this case the multi-stage post-cure gave significantly higher strength at -55°C. This difference between M3 and R1 is not understood.

5.2.2 Metal-CFRP joints

The theory presented earlier predicts that thermal mismatch stresses generated in the adhesive of metal-CFRP joints will give substantially lower strengths than for metal-metal joints, particularly at low temperatures. It was also shown that thermal mismatch stresses will be considerably less and joint strengths therefore greater for titanium-CFRP joints than for aluminium-CFRP joints. These predictions are largely borne out by the data summarised in Table 3.

However, reduction of cure temperature did not increase strengths of metal-CFRP joints tested at RT and -55°C, in contrast to the theoretical prediction, and in some cases gave lower strengths. This was most notable for adhesive E, where the reduction of 30 K in ΔT was nevertheless associated with falls in strength of 12% at RT and 37% at -55°C, which may be explained by assuming that a fully toughened structure did not develop during a 90°C cure. Nor did the use of cold-setting adhesives with multi-stage post-cures prove beneficial. Adhesive R1 gave particularly weak joints at -55°C, again probably because of its brittleness, and the alternative cures gave similar strengths.

The interpretation of results for adhesive M3 is clouded by the large scatter. As described in section 4.2 this was related to variable degrees of incomplete abrasion of the CFRP, and the cause was presumably residual PTFE on areas of incomplete abrasion[15,16]. A puzzling feature is that the CFRP for joints with adhesive C was grit-blasted and primed as part of the same batch as used for M3 yet adhesive C gave high strengths without excessive scatter. Close examination of these latter joints also revealed appreciable areas of AC failure that showed signs of incomplete abrasion, yet there was only a weak correlation between strength and proportion of AC failure, which was statistically significant only for joints cured 0.5 h at 120°C and tested at +80°C. Such contrasts between adhesives in their response to lack of abrasion have been observed elsewhere[17-19], and are unexplained as yet: the present example is even more surprising because the same primer was interposed between CFRP surface and adhesive for both adhesives.

Returning to consideration of adhesive M3, the two post-cure schedules gave similar mean strengths at any test temperature; and regression lines of RT strengths versus proportion of AC failure for the two cures extrapolated to zero AC failure predicted strengths of 33.8 MPa for the single-stage post-cure and 34.7 MPa for the multi-stage cure, not a significant difference. (The regressions at -55°C did not give significant correlation coefficients.) Thus, again a reduced cure temperature does not appear to give higher strengths.

5.2.3 Effect of adhesive mechanical properties on the strength of metal-CFRP joints

Comparing adhesives, it is clear that some of the metal-CFRP joints are much stronger, particularly at low temperature, than predicted by the simple theoretical analysis outlined in section 2, as would be expected because non-linear and inelastic behaviour of the adhesive were ignored. Although these contrasts between adhesives cannot be fully understood without the application of complex stress analyses, it is possible to advance qualitative explanations for some of the major differences in strengths. Adhesives B and C in particular provide interesting contrasts in low temperature strength because they are of similar general character, with similar T_d, shear strength and elastic modulus. Their shear stress-strain curves are reproduced in Figs 7 and 8, redrawn from Ref 10 to a uniform strain scale and showing the derived values of initial tangent modulus, failure stress and failure strain at RT and -55°C. The main difference between these two adhesives is that B has a much higher strain to failure. It is postulated that this higher strain capability permits a larger fraction of the adhesive layer to carry high stress when peak stress and strain at the critical overlap end reach ultimate. A purely qualitative illustration of this (not based on any actual stress analysis) is shown in Fig 9. In Fig 9a the solid lines indicate the regions of the stress-strain curves within which the two adhesives are assumed to be working at the moment of failure at -55°C. Fig 9b shows the corresponding stress distribution along the overlap length of metal-CFRP joints, due to the combined effect of applied load and thermal mismatch. It is clear that at -55°C adhesive B will give a higher *average* stress than adhesive C, despite the latter having a higher *failure* stress. Differences in joint strengths between adhesives B and C will be much less at RT because the contribution of thermal strain to total strain is much smaller. It is therefore suggested that at the point of failure at RT both adhesives are working wholly within the ductile regions of their stress-strain curves; they will be undergoing plastic deformation along the entire overlap with almost constant stress, resulting in similar average stresses for the joints. Another difference between these two adhesives is that for adhesive C the stress-strain curve reaches a plateau and then turns over at high strains (Fig 8). The significance of this is uncertain, but if it indicates rapid creep just prior to failure this may also contribute to the lower strengths observed for this adhesive. In contrast, for adhesive B stress increases continuously with strain until failure occurs (Fig 7).

Adhesive R1 gave outstanding strengths at RT. This adhesive exhibits unusually high strain to failure and low initial modulus at RT, although the maker's data is insufficiently detailed to give precise values[20]: failure strain was in the range 1.7 to 3.2, initial modulus 52-97 MPa, and failure stress 47.9 MPa. These data are for a cure at RT only; the post-cure used in the present work would raise strength and modulus, and probably reduce failure strain, but nevertheless this adhesive would remain unusually ductile at RT. From the simple elastic analysis of section 2 it can be seen that low adhesive modulus G favours the attainment of higher strength P for a given ultimate stress τ (equation (3)), consistent with the observed result. The behaviour at -55°C

is in complete contrast. No stress-strain curve is available but the low lap shear and peel strengths of metal-metal joints at low temperature (this work and Ref 20) indicate that the adhesive is much more brittle.

For the joint geometry and materials used in the present work failures were probably induced mainly by peel stresses at the ends of the outer adherends. It is shown in Appendix A, section A.3 that if the adhesives develop their maximum plastic shear strength near the end of the overlap then peel stresses would considerably exceed composite TTS. Thus it appears that the *combination* of thermal stress and relatively low composite TTS caused the metal-CFRP joints to be weaker than the corresponding metal-metal joints. This is consistent with failure occurring largely within the composite. The differences in failure mode shown in Table 5 presumably reflect the relative values of composite TTS and adhesive tensile strength. Adhesive B, which gave considerable CA failure, has a tensile strength not much higher than the composite (see Appendix A). Data for the other adhesives are not available but it may be surmised that adhesives C and E have tensile strengths substantially higher than the composite. Adhesive R1 is perhaps an unusual case where the primer layer or the primer/adhesive interface seem to be the weakest regions.

Finally, it is clear that prediction and interpretation of joint strengths requires full mechanical property data for adhesives, coupled with application of stress analyses that include both differential thermal contraction and elastic-plastic behaviour of the adhesive as minimum requirements. The role of low composite TTS is also evident, but its importance will vary considerably with joint geometry: thus scarf and multi-step lap joints will be less affected by peel stresses. Data obtained with the conventional single or double lap joint cannot be directly applied to other geometries without an understanding of the differing stress distributions.

6 CONCLUSIONS

(1) Metal-CFRP joints were weaker than mechanically similar metal-metal joints, particularly at low temperature. This was due to the combined effects of differential contraction of adherends in metal-CFRP joints and the relatively low TTS of CFRP.

(2) The ratio of metal-CFRP to metal-metal joint strengths at $-55^{\circ}C$ varied widely according to the adhesive, with a ductile adhesive giving a high ratio.

(3) Reduction of thermal stress by substituting titanium for aluminium considerably increased strengths of metal-CFRP joints at low temperature.

(4) Reduction of stress-free temperature by lowering cure temperature did not increase strength of metal-CFRP joints.

(5) Fuller mechanical property data for adhesives, allied to more thorough stress analyses, are needed to establish the relationship between adhesive characteristics and strength of joints.

Appendix A

STRESSES IN THE ADHESIVE
(List of symbols section 2.1)

A.1 Introduction

This analysis of joint stresses is confined to simple approximate methods which indicate the important parameters and their influence on joint strength. The most important approximations are the assumption of linear elastic behaviour for the adhesive (neglecting the extended ductile behaviour of typical toughened adhesives, see Figs 7 and 8), and neglect of shear strain in the composite. Both approximations will tend to overestimate the shear stresses in the adhesive of the ends of the overlap.

A.2 Shear stresses

Ref 7 presents a typical shear lag analysis, in which the following simplifying assumptions are made:

(i) adherends are homogenous and isotropic or orthotropic;

(ii) adherends and adhesive are linearly elastic;

(iii) shear strain in the adhesive at any point is uniform through its thickness;

(iv) only axial strains in the adherend are considered;

(v) bending of the adherends is neglected.

Referring to Fig 1 the distribution of adhesive shear stress in the x direction is given by equation (A1.5) of Ref 7

$$\tau = \frac{PG}{bdE_1t_1K' \sinh K'\ell}\left[\frac{E_1t_1}{E_2t_2}\cosh K'x + \cosh K'(\ell - x)\right] + \frac{\Delta\alpha\Delta TG}{dK' \sinh K'\ell}\left[\cosh K'x - \cosh K'(\ell - x)\right] \qquad \text{(A-1)}$$

where $K' = \sqrt{\frac{G}{d}\left(\frac{1}{E_1t_1} + \frac{1}{E_2t_2}\right)}$.

In the present work the adherend thicknesses were chosen so that adherends 1 and 2 were approximately stiffness balanced, *ie* $E_1t_1 \simeq E_2t_2 = (Et)$. Thus

$$K' \simeq \sqrt{\frac{2G}{d(Et)}} = K$$

and equation (A-1) simplifies to

$$\tau = \frac{PG}{bd(Et)K \sinh K\ell}\left[\cosh Kx + \cosh K(\ell - x)\right] + \frac{\Delta\alpha\Delta TG}{dK \sinh K\ell}\left[\cosh Kx - \cosh K(\ell - x)\right] \qquad \text{(A-2)}$$

With metal outer adherends (2) and composite central adherend (1), tensile applied load, and actual temperature below the stress-free temperature the end x = 0 becomes critical because thermal and load stresses are the same sign at this point.

Substituting K and $x = 0$ into equation (A-2) and re-arranging we have for the peak shear stress in the adhesive at this end of the overlap

$$\tau_{max} = \frac{P}{2b}\sqrt{\frac{2G}{d(Et)}}\left[\frac{1 + \cosh K\ell}{\cosh K\ell}\right] + \Delta\alpha\Delta T\sqrt{\frac{G(Et)}{2d}}\left[\frac{1 - \cosh K\ell}{\sinh K\ell}\right] . \qquad (A-3)$$

For the materials and joint dimensions used in the present work it can be shown that $K\ell \simeq 4$, thus $\cosh K\ell \simeq \sinh K\ell \simeq 27.3$ and the terms in square brackets in equation (A-3) are to a good approximation 1 and -1 respectively. Thus

$$\tau_{max} \simeq \frac{P}{2b}\sqrt{\frac{2G}{d(Et)}} - \Delta\alpha\Delta T\sqrt{\frac{G(Et)}{2d}} . \qquad (A-4)$$

The materials properties and joint dimensions relevant to the present work are summarised in Table A1, the value of G being typical for a toughened epoxy adhesive. For aluminium alloy-CFRP joints a mean value of (Et) is taken as 0.134 GN/m. The term $K\ell$ then becomes 4.04, leading to the simplification above.

Table A1

Materials properties and joint dimensions for the estimation of peak stresses in the adhesive

Property and units	Aluminium alloy	Titanium alloy	CFRP	Adhesive
ν	0.33	0.31	-	-
E (GPa)	72	110	129*	-
t (mm)	$t_2 = 2$	$t_2 = 1.2$	$t_1 = 0.965$*	-
Et (GN/m)	0.144	0.132	0.124	-
α (K^{-1})	22×10^{-6}	8×10^{-6}	-0.2×10^{-6}	-
G (GPa)	-	-	-	0.7
d (mm)	-	-	-	0.1
ℓ (mm)	12.5 in all cases			

* extrapolated to 60% fibre volume fraction: see Appendix B, section B.4.

The importance of thermal stress can be illustrated by sample calculations using equation (A-4). Stress-free temperature is assumed to be 95°C and operating temperature either -55°C or +10°C, so that ΔT is either -150 K or -85 K. In the latter case assume that an external load 2P of 3.6 kN is also present, *ie* about 15% of ultimate strength at RT of most joints in this work. The outcome is summarised in Table A2, which shows the very high thermal stresses in aluminium alloy-CFRP joints. These are of course substantial overestimates because of neglect of adhesive ductility and creep, but nevertheless the preponderance of thermal stress is striking. In contrast, the peak shear stresses calculated for titanium-CFRP joints remain within, or almost within, the elastic region for typical adhesives (Figs 7 and 8).

Table A2

Estimate of peak shear stresses in the adhesive layer of metal-CFRP joints due to differential thermal contraction of adherends and external load

Property and units	Aluminium alloy-CFRP joint		Titanium alloy-CFRP joint	
	$\Delta T = -150$ K, $2P = 0$	$\Delta T = -85$ K, $2P = 3.6$ kN	$\Delta T = -150$ K, $2P = 0$	$\Delta T = -85$ K, $2P = 3.6$ kN
$\Delta\alpha$ (K^{-1})	22.2×10^{-6}		8.2×10^{-6}	
Mean (Et) (GN/m)	0.134		0.128	
$L^{\tau}max$ (MPa)	0	11.6	0	11.9
$T^{\tau}max$ (MPa)	72.1	40.9	26.0	14.8
τ_{max} (MPa)	72.1	52.5	26.0	26.7

A.3 Peel stresses as a cause of joint failure

Hart-Smith[8] pointed out that failure of composite joints is likely to be caused by peel stresses (normal to the plane of the joint) at the ends of the outer adherends: i.e. failure will tend to occur in the composite because of its relatively low TTS compared to tensile strengths of toughened adhesives. The approximate treatment described in Ref 8 assumes the following characteristics for the joint under high load just before failure.

(a) Shear ductility of the adhesive gives an almost constant shear stress near the end of the joint.

(b) In contrast, the adhesive in normal tension behaves elastically because the relatively rigid adherends constrain the thin adhesive layer laterally.

Applying plate bending theory to the outer adherends Hart-Smith showed (equation (83) of Ref 8) that the peel stress is given by

$$\sigma = \tau \left[\frac{3E'_A \left(1 - \nu_2^2\right) t_2}{E_2 d} \right]^{\frac{1}{4}} . \qquad \text{(A-5)}$$

(This applies for sufficiently long overlaps, a condition satisfied by the joints used in the present work.)

E'_A is the Young's modulus applicable to a thin adhesive layer constrained by the adherends, and will be considerably higher than the modulus as usually measured. The only data available on materials used in the present work are for adhesive B at RT with a thickness of 0.14 mm[9]. E'_A was found in a butt tensile test to be about 3-6 times the unconstrained modulus; there was much scatter with values ranging from 5.9 to 11.7 GPa. Let us assume an approximate mean of 9 GPa. To determine peel stress at the point of

failure we set τ in equation (A-5) equal to the adhesive shear strength, and this shear stress is assumed to be constant near the overlap end, as required by the theory. This is a reasonable assumption, because in the present work aluminium-aluminium joints for adhesive B gave a RT strength (*ie* an average shear stress) of 45.4 MPa (Table 3), in good agreement with the pure shear strength of 45 MPa determined by Althof *et al*[10]. This implies that at failure the whole adhesive layer was in the fully plastic state, with shear stress almost constant along the whole overlap length. We therefore insert a value of 45 MPa for τ in equation (A-5); other parameters are listed in Table A1.

The following values of σ were then calculated from equation (A-5):

for an aluminium alloy-CFRP joint σ = 72.4 MPa;
for a titanium alloy-CFRP joint σ = 57.5 MPa.

These stresses are well above the composite TTS of 39.4 MPa (Table B1). (This was as usual measured in the plane of the laminate but the normal-to-plane strength would not be greatly different.) They are also higher than the tensile strength of adhesive B, for which rather discrepant values appear in the literature: Ref 9 gives a range of 35.1 to 46.9 MPa but some of these were probably low due to voidness, while values of 52.4 and 54.2 MPa were obtained elsewhere[21,22]. The estimate of σ therefore implies a tensile strength for this adhesive substantially higher than the cited values.

However, despite this discrepancy the constraint on joint strength imposed by low composite TTS is clear, and is consistent with observed joint failures being largely in the composite. It should be noted that in contrast the composite shear strength was 81.9 MPa, well above values for the adhesives.

Appendix B

PROCESSING AND PROPERTIES OF CFRP LAMINATES

B.1 Introduction

Because of the importance of composite shear and transverse characteristics in determining joint strengths and mode of failure the processing and properties are detailed here.

B.2 Material

This was supplied as prepreg sheets to Ministry of Defence Provisional Specification NM 547 by Fothergill and Harvey, and comprised Courtaulds Type 140 SC/10000 fibre to Provisional Specification NM 565 with matrix resin Fothergill and Harvey Code 91 (Shell Epikote DX 210 with hardener DX 137).

B.3 Processing

The prepreg was moulded into unidirectional boards, containing ten layers giving a nominal thickness of 2 mm and a fibre volume fraction of 60% using an autoclave cure of 2 h at 120°C. The layup was kept under vacuum until the temperature reached 60-70°C when a pressure of 1.24 MPa was applied. Release layers were PTFE-coated glass cloth which was removed shortly after completion of cure, and cured boards were then stored in unsealed polythene bags at ordinary ambient conditions.

B.4 Properties

Difficulty was experienced in achieving uniform thickness and fibre volume fraction presumably because of patchy ageing of the uncured resin and hence variable bleed out during cure: thickness ranged from 1.89 to 2.50 mm with corresponding variation of volume fraction from 49-61%. However, there was no correlation of joint or composite strength with laminate thickness, and it should be noted that regardless of thickness the laminate contained the same cross-sectional area of fibre so that the longitudinal tensile stiffness was almost independent of thickness.

Void and fibre contents were determined by chemical digestion[23]. (Composite density was determined by weighing and measuring the samples because density bottle measurements proved to be inaccurate.) The general void content was low (see Table B1), but there were isolated larger voids usually close to the laminate mid-plane, which tended to occur in bands (detected by ultrasonic C-scanning) and were often related to the patchy thickness variations noted above. For manufacture of joints the edge to be bonded was chosen so as to minimise the number of these visible voids in the bond areas: it was later found that in fact the presence of a void did not initiate composite failure when joints were tested, nor were such joints weaker than average.

Properties of the cured laminate are summarised in Table B1. Longitudinal mechanical properties were measured by the prepreg suppliers on their samples. Interlaminar shear strength (ILSS) and transverse tensile strength (TTS) were measured by standard methods[23] on several specimens taken from widely distributed points on each of

the six boards. Only values from specimens free of visible voids were included. The ILSS and TTS compare well with makers' data and other published values[24,25].

Table B1

Properties of cured CFRP laminates

Property and units	Board number						Overall value
	7/1	8/1	9/1	9/2	10/1	10/2	
Flexural strength (GPa)	-	-	-	-	-	-	(3) Note 2 1.44
Flexural modulus (GPa)	-	-	-	-	-	-	(3) Note 2 129
ILSS at RT (MPa)	(4) 84.5 1.45	(5) 80.3 1.10	(5) 82.0 1.45	(5) 80.6 3.63	(5) 84.3 1.66	(5) 80.2 3.36	(29) 81.9 2.80
ILSS at 80°C (MPa)	(5) 53.5 1.18	(4) 51.5 1.32	(5) 51.2 0.66	(5) 50.3 2.17	(5) 54.6 0.51	(5) 52.8 1.01	(29) 52.4 1.90
TTS at RT (MPa)	(3) 39.6 2.76	(4) 37.6 7.51	(4) 36.8 2.52	(5) 39.2 8.27	(5) 42.8 3.24	(3) 39.3 0.62	(24) 39.4 5.19
TTS at 80°C (MPa)	(4) 31.0 2.48	(5) 32.2 1.93	(5) 37.2 5.44	(5) 29.5 1.99	(5) 24.5 8.42	(5) 26.9 2.90	(29) 30.2 5.88
Void content (%)	(3) 1.8 0.21	(3) 0.8 0.10	(3) 1.1 0.59	(3) 1.9 0.45	(3) 0.8 0.21	(2) 2.0 0.78	(17) 1.35 0.62
Fibre volume fraction (%)	(3) 55.4 2.16	(3) 57.4 3.80	(3) 58.5 2.72	(3) 56.8 2.52	(3) 58.1 2.44	(2) 55.6 3.11	(17) 57.0 2.62

NOTES : (1) The values in each box are, respectively: number of samples (in brackets), mean, standard deviation.

(2) Actual fibre volume fraction was 56%, values were extrapolated to 60%; values from prepreg suppliers.

Appendix C

SURFACE PRETREATMENT AND PRIMING OF ADHERENDS

C.1 Introduction

Because of the potential importance of surface pretreatment in determining strength and durability of joints full details are given here. Pretreatments chosen were intended to be representative of actual or likely future industrial practice, but close control was exercised to reduce variability of prepared surfaces.

C.2 Pretreatment for aluminium alloy

During storage and machining the soft cladding layer was protected from scratching and corrosion by tissue paper stuck on with oil.

C.2.1 Precleaning

Plates were allowed to soak for up to 1.5 h in a solvent mixture and then gently swabbed with tissues to remove oil and identification marks. Initially the solvent mixture was one part by volume white spirit (BS 245) to two parts propan-2-ol, but the latter solvent was later changed to 2-ethoxy ethanol for easier removal of identification paint. Plates were then vapour degreased in 1,1,1-trichloroethane, and closely wrapped in clean paper for storage. The final stage of cleaning was an aqueous alkaline degrease, which immediately preceded the aqueous preparation stages described below. For this and subsequent stages the plates were mounted in screw clips in a rack. The degreasing solution was Minco 3410 (W. Canning and Co Ltd) a non-silicated, non-caustic, mildly alkaline cleaner, used at a concentration of 32-40 g/l, and immersion was for 5 min at 63-67°C. Plates were immediately washed in cold tap water (see below for details of washing) and proceeded directly to the next stages.

C.2.2 Etching and anodising

Etching was carried out in a chromic acid/sulphuric acid bath according to Method O of DEF-STAN 03-2/1 for 30 ± 1 min at 61-64°C. The actual bath composition (in g/l) on completing the whole batch of plates was:

Cr^{VI} as CrO_3	43.9
Cr^{III} as CrO_3	27.5
H_2SO_4	320.3
Al	6.5
Cu	0.1 .

Industrial grades of CrO_3 and H_2SO_4 were used.

Plates were then washed twice in cold tap water (see below) and normally passed directly to the anodise stage without being dried. (In one case it was necessary to dry as described below and complete the work next day; these pickled plates remained in the rack and were kept in a closed container.)

Anodising was in phosporic acid essentially to Boeing Process Specification 5555. Analar phosphoric acid was used and the concentration on completing the whole batch was 104.5 g/l, with 0.8 g/l of aluminium dissolved from the plates. Temperature was 25 ± 1°C, time 22-23 min, voltage 10 ± 0.5 V and current density typically around 20 A m^{-2}. The cathodes were stainless steel (BS S526) and the anode/cathode area ratio 3.5 to 4:1. Using the polarised light test described in the Boeing specification it was found that panels tended to give more intense colours near their ends, suggesting thicker anodic oxide in these areas, but this had no apparent effect on joint strength. The panels passed immediately to the first wash with no delay longer than 1 min (see below).

C.2.3 Washing

This description applies to all the washing stages noted above. Washing was carried out in a specially cleaned sink which was emptied, hosed-down and refilled before each wash stage. The local mains water was used at its natural temperature (10-15°C); this water is a mixture of variable composition drawn from several sources some of which are softened by the base exchange process. Typical compoeition ranges (mg/l) are:

pH	7.4 - 8.5
Total dissolved solids	165 - 350
Ca	75 - 97
Na	34 - 45
CO_3^{2-}	61 - 162
SO_4^{2-}	11 - 13
Cl	14 - 19
NO_3^-	7 - 12
SiO_2	15 - 22
F^-	Approx 0.1 .

After each of the aqueous processes the panels were given a first wash of 1-2 min to remove the majority of the previous treatment solution: they were immersed in clean flowing water which was then drained off while the plates were hosed down. (This was the sole wash step after Minco cleaning.) For the second wash after etching and anodising the sink was re-filled and the panels allowed to stand in flowing water for 20 ± 2 min.

C.2.4 Drying, priming and storage

Drying was for 15 ± 1 min in a fan circulated oven preheated to 58-62°C, although the plates did not attain the full temperature in that time. The oven had been thoroughly cleaned and was reserved solely for this purpose. The plates were mounted so that water drained away from the edges to be bonded.

Plates were then removed from the handling rack and placed between layers of Melinex film for temporary storage until priming, which was done within 4.6 h of completing drying. Primers were sprayed on in several thin coats to minimise thickness

variations, to an estimated coating thickness of 2-3 μm as judged against colour standards. Care was taken to avoid local heavy coverages with chromate pigment, which was prevented from settling in the spraygun reservoir. Primers were allowed to air-dry for at least ½ h, and Primer 2 was additionally dried at 70°C for 30 min as recommended; both primers were finally cured at 120°C for 1 h. (For some batches this was done several days later, in which case the plates were wrapped in Melinex film for temporary storage.) Primed plates were wrapped in Melinex film for storage and if not used within 3 weeks were also sealed in polythene bags containing silica gel.

C.3 Pretreatment for titanium alloy

This was the RAE 65°C alkaline peroxide etch[4].

C.3.1 Precleaning

Solvent swabbing was as for aluminium-alloy, but vapour degreasing was omitted. An additional stage was wet alumina grit blasting (180 grade), which was found in trials to be essential for consistent etching and good joint durability; grit and debris were removed by brushing in cold tap water and the panels air-dried. Minco treatment followed 1 or 2 days later as for aluminium, and washing was as described earlier.

C.3.2 Alkaline peroxide etch

This was done immediately following the wash after Minco treatment. Fresh solutions were made up for each treatment batch to the following composition, with the hydrogen peroxide added just before immersing the plates:

NaOH	20 g/l
H_2O_2(100 vol)	22.5 ml/l .

It was necessary to divide the work between three small tanks which were heated by an outer tank of water, and this led to temperature differences between tanks of up to 5 K; the vigour of the reaction also caused a temperature increase during etching of up to 2 K, so that overall the temperature range was 61-68°C. Also, one of the tanks was stainless steel while the others were polythene coated, and the former gave a higher rate of H_2O_2 decomposition and slightly different colour to the etched plates. However, there was no consistent difference in joint strengths between panels that had passed through different tanks.

Etch time was 20-23 min and washing followed within ½ min.

C.3.3 Washing and de-smutting

The washing was essentially as described for aluminium alloy, except that first and second washes were in separate stainless steel tanks. However, it was necessary to introduce a de-smutting stage in which the panels were scrubbed vigorously with a stiff brush while in the first wash. The smut consisted of a thin layer of white particles, which in trials produced variable coverage from nil up to about 75% of the surface. The coverage by particles after brushing in these two production batches ranged from 5-25%. The presence of some smut is not believed to seriously affect joint strength or

durability[26], and in the present work there was no evidence that the two treatment batches gave different results although Batch I had more residual smut.

C.3.4 Drying, priming and storage

This was as described for aluminium alloy.

C.4 Pretreatment for CFRP

The CFRP had been moulded against PTFE-coated glass-cloth so it was necessary to remove traces of PTFE that may have adhered to the resin[15,16]. Dry grit blasting was the most practicable method of attaining complete abrasion, and was used in preference to wet blasting because of the possible effects of water on the matrix resin and the resin-to-fibre bond. The aim was to abrade only the surface skin of matrix resin without breaking through to the fibres, in order to reduce the risk of fibre-to-metal contact in the joints: such contact would increase the likelihood of corrosion in joints subjected to weathering.

C.4.1 Precleaning

Panels were first wiped with tissues moistened with distilled water to remove tap water deposits acquired during immersion in the ultrasonic scanning tank. Wax pencil marks were removed by local swabbing with propan-2-ol or 2-methoxyethanol, and panels were then brush washed all over with 2-butanone, air-dried and wrapped in Melinex film for storage.

C.4.2 Abrasion and solvent swabbing

Dry grit blasting was done with 280 grade alumina at pressures of 400 kPa to 600 kPa; the gun was positioned about 140 mm from the panels which were traversed through the grit stream at about 150 mm/s in a single movement. (In trials these conditions gave complete coverage with abrasion pits but without exposure of substantial proportions of carbon fibre. In the production batches there was greater variability in degree of abrasion, and up to about 25% of the surface was exposed fibre; this caused variable joint strengths only with adhesive M3 as discussed in section 4.2 and shown in Figs 4 to 6.)

Within 6 h of blasting the panels were cleaned with a short, fine-haired brush while immersed in 2-butanone; this process was then repeated with fresh solvent. (Panels were held with forceps and clean rubber gloves were worn.) They were drained and air-dried with bonding edges uppermost.

C.4.3 Priming and storage

This was as described for aluminium, with primer applied no later than 2 h after completion of swabbing.

Table 1

COEFFICIENTS OF LINEAR THERMAL EXPANSION FOR CFRP AND COMMON AEROSPACE STRUCTURAL METALS

Material	CFRP layup orientation	Direction of measurement relative to fibres	Coefficient of expansion (10^{-6} K^{-1})
CFRP	Unidirectional	0^{o}	-0.2
	0, 90^{o}	0^{o}	3
		45^{o}	3
	0, $\pm 45^{o}$	0^{o}	-0.3
		90^{o}	7
Aluminium	-	-	22
Steels S524	-	-	16
S534	-	-	12
Titanium	-	-	8

(Note : Typical average values at around ambient temperature, CFRF values do not refer to any particular material.)

Table 2

T_d VALUES FROM TMA MEASUREMENTS ON CURED ADHESIVES[11,12]

Adhesive	Cure or post cure cycle (hours and °C)	T_d (°C)
B	1/120	102
	6/90	99
C	0.5/120	95
	4/90	96
E	1/120	120
	6/90	114
M3	2/100	100
	4/40 + 4/60 +1/80 + 1/100	100
R1	1/80	102
	1/40 + 1/60 + 1/80	104

Table 3

DOUBLE LAP SHEAR STRENGTHS OF METAL-METAL AND METAL-CFRP JOINTS : EFFECT OF CURE CYCLE AND TEST TEMPERATURE

Adhesive, metal	Cure cycle (h/°C)	Test temp (°C)	Joint strength and coefficient of variation (CV)				Strength ratio, metal-CFRP to metal-metal (%)
			Metal-metal		Metal-CFRP		
			Strength (MPa)	CV (%)	Strength (MPa)	CV (%)	
B, Al	1/120	+80	-	-	23.2	4.4	-
		RT	45.4	2.4	37.6	5.6	82.8
		-55	62.9	3.4	39.0	9.7	62.0
	6/90	+80	-	-	25.6	4.2	-
		RT	47.8	1.4	39.6	2.6	82.8
		-55	53.3	2.7	29.5	7.4	55.3
C, Al	0.5/120	+80	-	-	26.0	3.2	-
		RT	44.8	1.7	35.7	9.5	79.7
		-55	61.9	1.3	11.0	40.7	17.8
	4/90	+80	-	-	26.6	5.8	-
		RT	46.0	0.9	33.2	13.3	72.2
		-55	61.8	0.7	12.0	39.3	19.4
C, Ti	0.5/120	+80	-	-	28.5	2.7	-
		RT	46.7	1.0	41.4	8.0	88.7
		-55	65.8	1.3	28.9	15.9	43.9
	4/90	+80	-	-	-	-	-
		RT	47.6	1.4	40.7	7.1	85.5
		-55	67.0	1.4	27.2	13.0	40.6
E, Al	1/120	+80	-	-	29.0	2.8	-
		RT	50.7	1.7	38.1	9.9	75.1
		-55	58.0	3.6	19.7	18.5	34.0
	6/90	+80	-	-	30.8	2.3	-
		RT	45.1	0.6	33.6	7.1	74.5
		-55	51.8	1.9	12.5	19.1	24.1
M3, Al	(a) 2-stage	+80	-	-	27.0	7.6	-
		RT	53.4	2.5	26.1 (b)	23.5	48.8
		-55	58.6	7.6	12.4	54.0	21.2
	(a) 5-stage	+80	-	-	26.8	2.1	-
		RT	53.6	2.1	26.8 (b)	21.9	49.9
		-55	43.6	15.5	7.4	38.0	17.0
RI, Al	(a) 2-stage	+80	-	-	22.9	5.1	-
		RT	57.2	4.7	47.9	12.3	83.7
		-55	37.2	5.1	6.0	20.8	16.1
	(a) 4-stage	+80	-	-	21.5	8.5	-
		RT	55.6	2.1	43.4	8.9	78.1
		-55	41.1	8.9	5.3	13.2	12.9

NOTES : (a) Refer to Table 2 for details
(b) Mean of 17 values, see section 4.2

Table 4

MODES OF FAILURE IN METAL-METAL JOINTS

Adhesive, metal	Cure cycle (h/°C)	Test temp (°C)	Percentage of lap area showing various modes of failure(a)		Notes
			AM	CA	
B, Al	1/120	RT	5	95	(b)
		-55	5	95	
	6/90	RT	5	95	(b)
		-55	5	95	
C, Al	0.5/120	RT	10	90	(c) (d)
		-55	10	90	
	4/90	RT	10	90	(c) (d)
		-55	10	90	
C, Ti	0.5/120	RT	10	90	(e)
		-55	10	90	
	4/90	RT	10	90	(e)
		-55	10	90	
E, Al	1/120	RT	5	95	(f)
		-55	5	95	
	6/90	RT	-	100	(f)
		-55	-	100	
M3, Al	2-stage	RT	-	100	(g)
		-55	-	100	
	5-stage	RT	-	100	(h)
		-55	-	100	
R1, Al	2-stage	RT	-	100	(i)
		-55	-	100	
	4-stage	RT	-	100	(i)
		-55	-	100	

KEY (see section 4.2) : AM = adhesion to metal, CA = cohesive within the adhesive layer.

NOTES : (a) Overall average for the set of replicates.
(b) 5-20% of the CA failure was close to the metal surface, either just outside the primer/adhesive interface or at this interface; there was more of such failure at -55°. Difficult to estimate true proportion of AM failure.
(c) About 50% of the CA failure was close to the metal surface as described under (b). Difficult to estimate true proportion of AM.
(d) 80-100% of the CA failure was close to the surface of the central adherend, as described above. Difficult to estimate true proportion of AM failure.
(e) Similar to (c) but about 60-80% of CA failure was close to interface on RT samples and 80-90% on -55°C samples.
(f) Most of the adhesive was retained on the outer adherend, particularly for joints tested at -55°C.
(g) 60-80% of the failure was in the region of the primer/adhesive interface on the central adherend in the samples tested at RT, and 80-100% on those tested at -55°C.
(h) 70-100% of the failure was in the region of the primer/adhesive interface, mainly on the central adherend, and in many cases the adhesive appeared to have debonded cleanly from the primer layer.
(i) Failure was in the adhesive, mainly close to the primer/adhesive interface on the central adherend, 70-90% for the RT samples and entirely for the -55°C samples.

Table 5

MODES OF FAILURE IN METAL-CFRP JOINTS

Adhesive, metal	Cure cycle (h/°C)	Test temp (°C)	Percentage of lap area showing various modes of failure[a]				
			AC	AM	CA	CC	Notes
B, Al	1/120	+80	0-10	-	70-90	5-30	
		RT	0-20	-	40-90	10-50	
		-55	0-25	-	5-20	70-90	(b)
	6/90	+80	-	-	80-95	5-20	
		RT	-	-	20-80	20-80	
		-55	0-5	-	0-10	90-100	(b)
C, Al	0.5/120	+80	0-20	-	0-5	80-100	(c)
		RT	0-30	-	-	70-100	
		-55	0-35	-	0-5	60-100	
	4/90	+80	0-30	-	0-20	50-100	(c)
		RT	0-20	-	5	50-95	
		-55	0-30	-	-	70-100	
C, Ti	0.5/120	+80	0-30	-	0-10	70-100	
		RT	0-10	-	0-5	85-100	
		-55	0-70	-	-	30-100	
	4/90	+80	Not available				
		RT	0-20	-	0-5	80-100	
		-55	0-40	-	-	60-100	
E, Al	1/120	+80	-	-	0-15	85-100	(b)
		RT	-	-	0-5	95-100	
		-55	-	-	-	100	
	6/90	+80	-	-	10-50	50-90	(b)
		RT	-	-	0-5	95-100	
		-55	-	0-5	0-10	85-100	
M3, Al	2-stage	+80	5-30	-	-	70-95	(c) and (e)
		RT	0-70	-	-	30-100	
		-55	0-80	-	-	20-100	
	5-stage	+80	5-40	-	10-50	10-80	(d) (e)
		RT	0-80	-	-	20-100	
		-55	0-100	-	-	0-100	
R1, Al	2-stage	+80	-	-	65	35	(b) (f)
		RT	-	-	20-95	5-80	
		-55	0-10	-	5-100	0-95	
	4-stage	+80	-	-	65	35	(f)
		RT	-	-	30-85	15-70	
		-55	0-10	-	90-100	0	

KEY (see section 4.2) : AC = adhesion to composite, AM = adhesion to metal, CA = cohesive within the adhesive, CC = cohesive within the composite, or within surface skin of composite.

NOTES : (a) This is an overall average or range for the set.
(b) The CA failure was more evident at the 'peel' end of the joint.
(c) The AC failure tended to be more evident at the 'peel' end of the joint.
(d) Part of the CA failure was at the primer/adhesive interface adjacent to the outer metal adherend.
(e) Strength was correlated with proportion of AC failure (see section 4.2).
(f) Much of the CA failure was close to the CFRP surface, either at the primer/adhesive interface or within the primer layer: the former location predominated on the -55°C samples.

REFERENCES

No.	Author	Title, etc
1	J.L. Cotter	The durability of structural adhesives. *Developments in adhesives*, edited by W.C. Wake, No.1, Chapter 1, pp 1-23, London, Applied Science Publishers (1977)
2	J.L. Cotter R. Kohler	The influence of surface pretreatment on the durability of adhesively-bonded aluminium alloys in humid and corrosive environments. *Int. J. Adhesion and Adhesives*, 1, 23-28 (1980)
3	E.W. Thrall	PABST programme test results. *Adhes. Age*, 22, Part 10, 22-33 (1979)
4	A. Mahoon J.L. Cotter	A new highly durable titanium surface pretreatment for adhesive bonding. In *Materials synergisms*, 10th National Technical Conference, pp 425-441, Society for the Advancement of Materials and Process Engineering, USA (October 1978)
5	A.R.G. Brown Donia E. Coomber	The electrochemical characteristics of carbon fibre reinforced plastic (CFRP) - aluminium alloy couples. RAE Technical Report 71247 (1971)
6	A.R.G. Brown Donia E. Coomber	The resistance to corrosion of some insulating carbon fibre reinforced plastic to aluminium alloy joints. RAE Technical Report 72160 (1972)
7	P. Grant	Strength and stress analysis of bonded joints. BAC MAD SOR(P) 109 (1976)
8	L.J. Hart-Smith	Adhesive bonded double-lap joints. NASA CR 112235 (1973)
9	W.J. Renton	Structural properties of adhesives, Vol.1. AFML-TR-78-127 (1978)
10	W. Althof G. Klinger G. Neumann J. Schlothauer	Klimaeinfluss auf die Kennwerte des elasto-plastichen Verhaltens von Klebstoffen in Metallklebungen. DLR-FB 77-63 (1977) [Available as "Environmental effects on the elastic-plastic properties of adhesives in bonded metal joints", translated by Barbara Garland; RAE Library Translation 1999 (1979)]
11	M.H. Stone	Effect of temperature and duration of cure on the heat distortion temperature, joint strength and durability of some structural adhesives bonded to aluminium. RAE Technical Memorandum Mat 318 (1979)

REFERENCES (continued)

No.	Author	Title, etc
12	M.H. Stone	The effect of adhesive properties on the low temperature strength of joints between metals and carbon fibre reinforced plastics. *Int. J. Adhesion and Adhesives*, 1, 203-207 (1981)
13	M.H. Stone	Effect of degree of abrasion of carbon fibre composite surfaces on strengths of adhesive bonded joints. RAE Technical Memorandum Mat 327 (1979)
14	M.H. Stone	Effect of degree of abrasion of composite surfaces on strengths of adhesively bonded joints. *Int. J. Adhesion and Adhesives*, 1, 271-272 (1981)
15	Brenda M. Parker	An X-ray photoelectron spectroscopic examination of surfaces of some thermosetting resins and carbon fibre composites. RAE Technical Memorandum Mat 347 (1980)
16	Brenda M. Parker R.M. Waghorne	Surface pretreatment of carbon fibre reinforced composites for adhesive bonding. *Composites*, 13, Part 3, 280-288 (1982)
17	P.K. Guha J.N. Epel	Adhesives for bonding graphite/glass composites. *Adhes. Age*, 22, Part 6, 31-34 (1979)
18	M.J. Davis A.A. Baker	Adhesive strength tests of bonded dissimilar materials using a step-lap sandwich specimen. ARL Mat. Note 113 (1976)
19	M. Dootson	The effects of surface treatment on the strength of CFRP tensile single lap joints for FM 96 and AF-127-3 adhesives. BAC MAD TN 4334 (1973)
20	B.F. Goodrich Co.	TAME - a new concept in structural adhesives. Information and data sheets (undated, about 1974)
21	H.C. Schjelderup W.B. Jones	Mechanical behaviour of cast adhesive film. *Adhes. Age*, 21 Part 2, 35-58 (1978)
22	B.J. Mulroy D.M. Mazenko	Adhesive bonding for space applications. In *Materials Synergisms*, 10th National Technical Conference, pp 416-424. Society for the Advancement of Materials and Process Engineering (1978)
23	J.B. Sturgeon	Specimens and test methods for carbon fibre reinforced plastics. RAE Technical Report 71026 (1971)
24	I.E. Hulme	Carbon fibre matrix evaluation programme. BAC(MAD) MDR 0039 (1976)

REFERENCES (concluded)

No.	Author	Title, etc
25	C.N. Owston	The effect of cure conditions on the mechanical properties of carbon fibre reinforced plastics. Cranfield Institute of Technology Fifth Report to Agreement AT/2028/058 MAT (1974)
26	J. Hamer	British Aerospace, Aircraft Laboratories, Weybridge, private communication (1978)

Reports quoted are not necessarily available to members of the public or to commercial organisations.

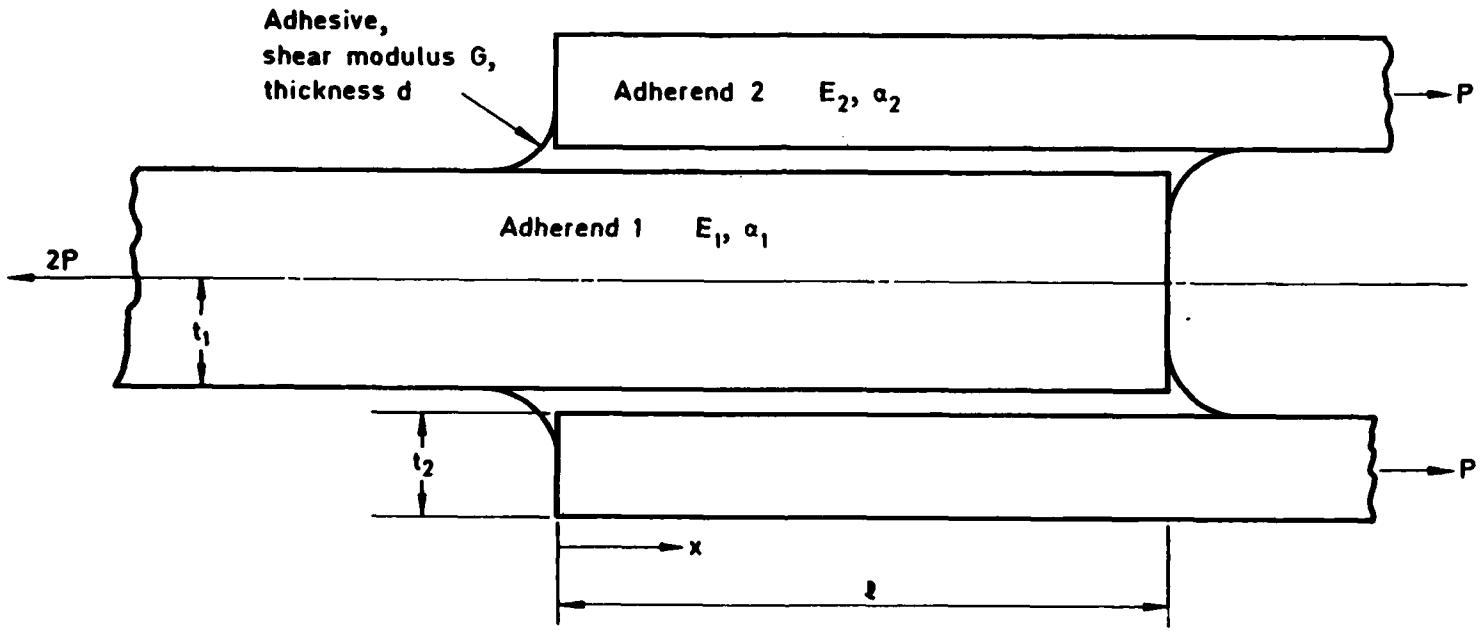

Fig 1 **Overlap region of symmetrical double lap shear joint**

For aluminium: $t_2 = 2\,mm$

$2t_1 = 4\,mm$

For titanium: $t_2 = 1.2\,mm$

$2t_1 = 2\,mm$

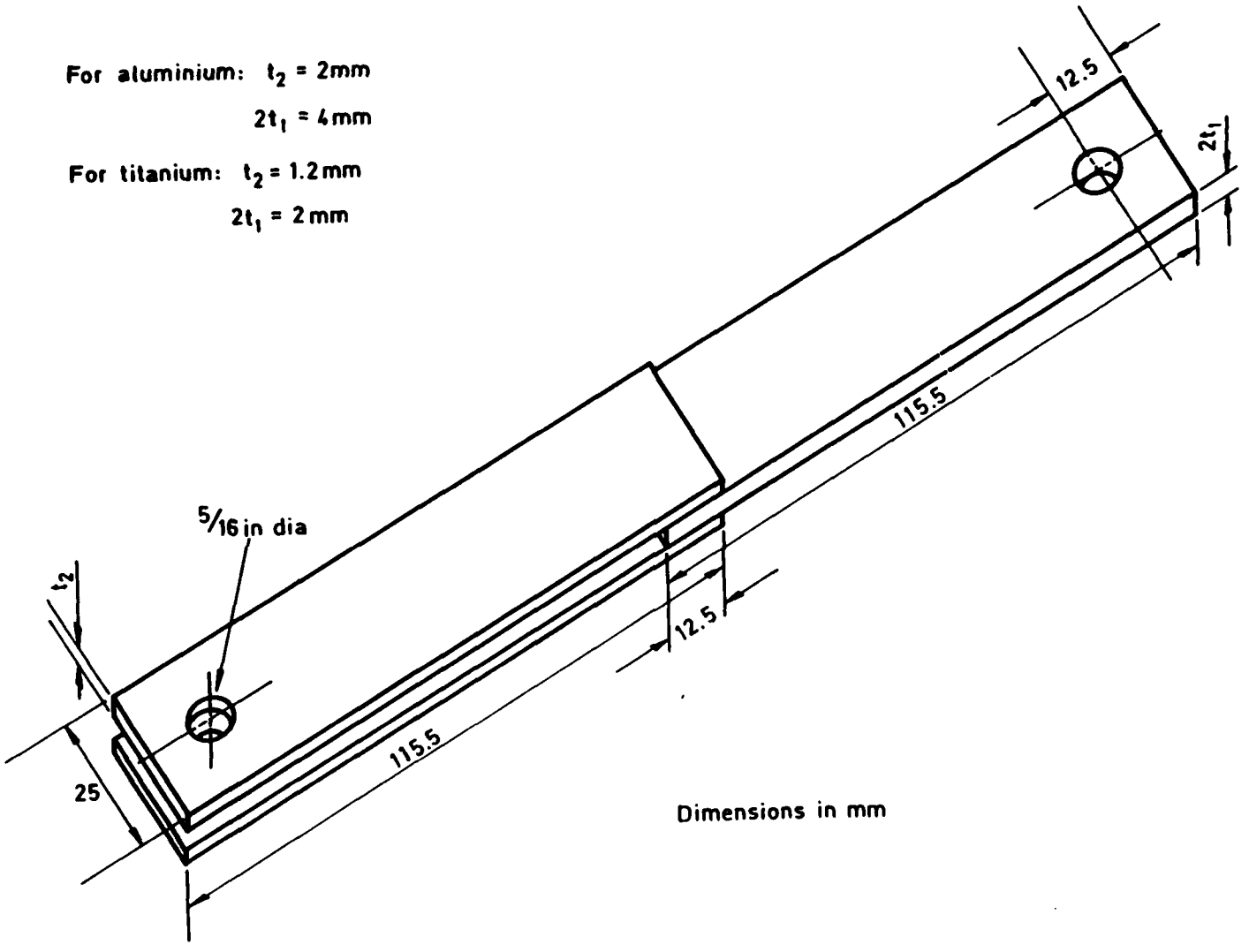

Fig 2 Adhesively bonded metal-to-metal symmetrical double lap joint

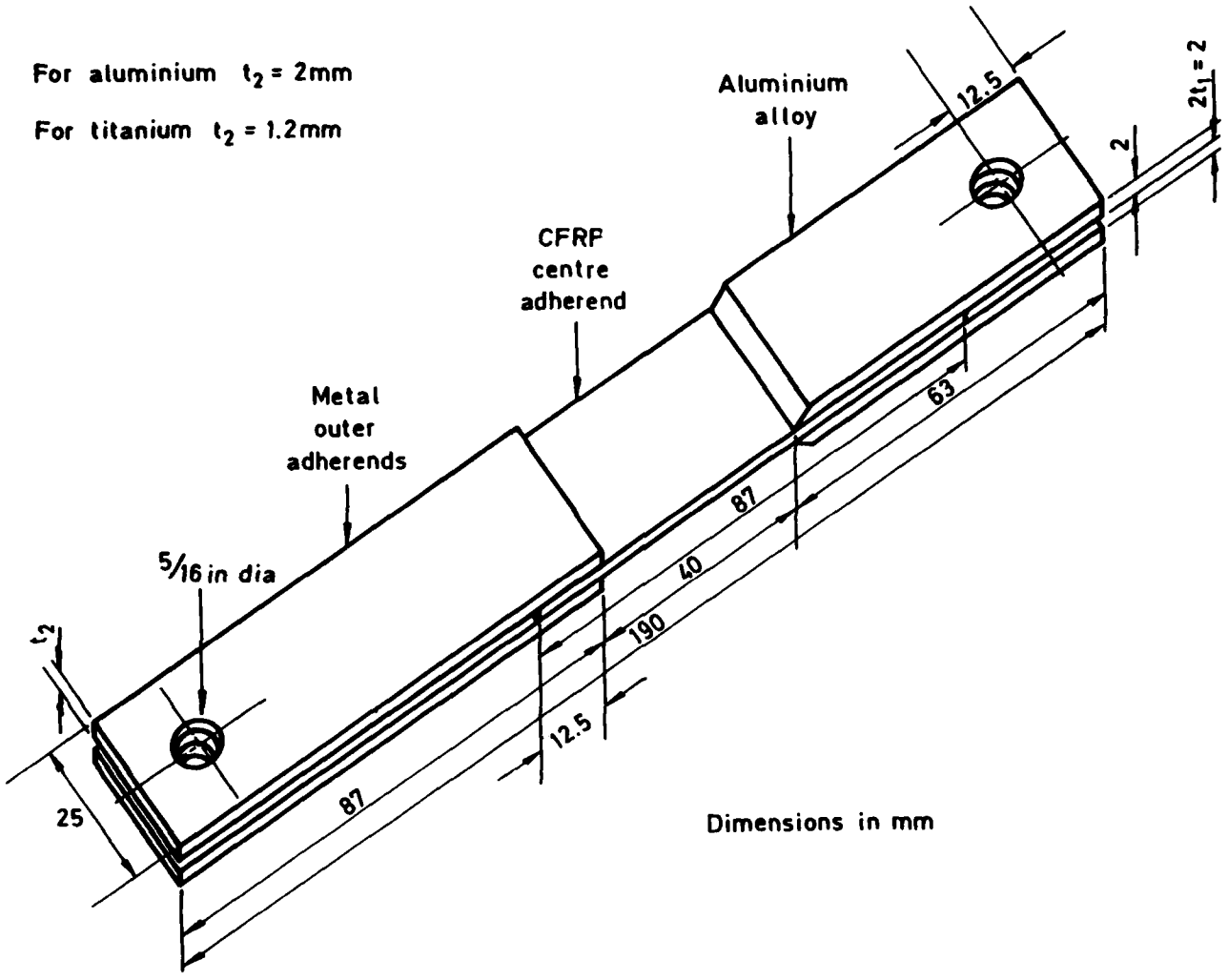

Fig 3 Adhesively bonded metal-to-CFRP symmetrical double lap joint

Fig 4

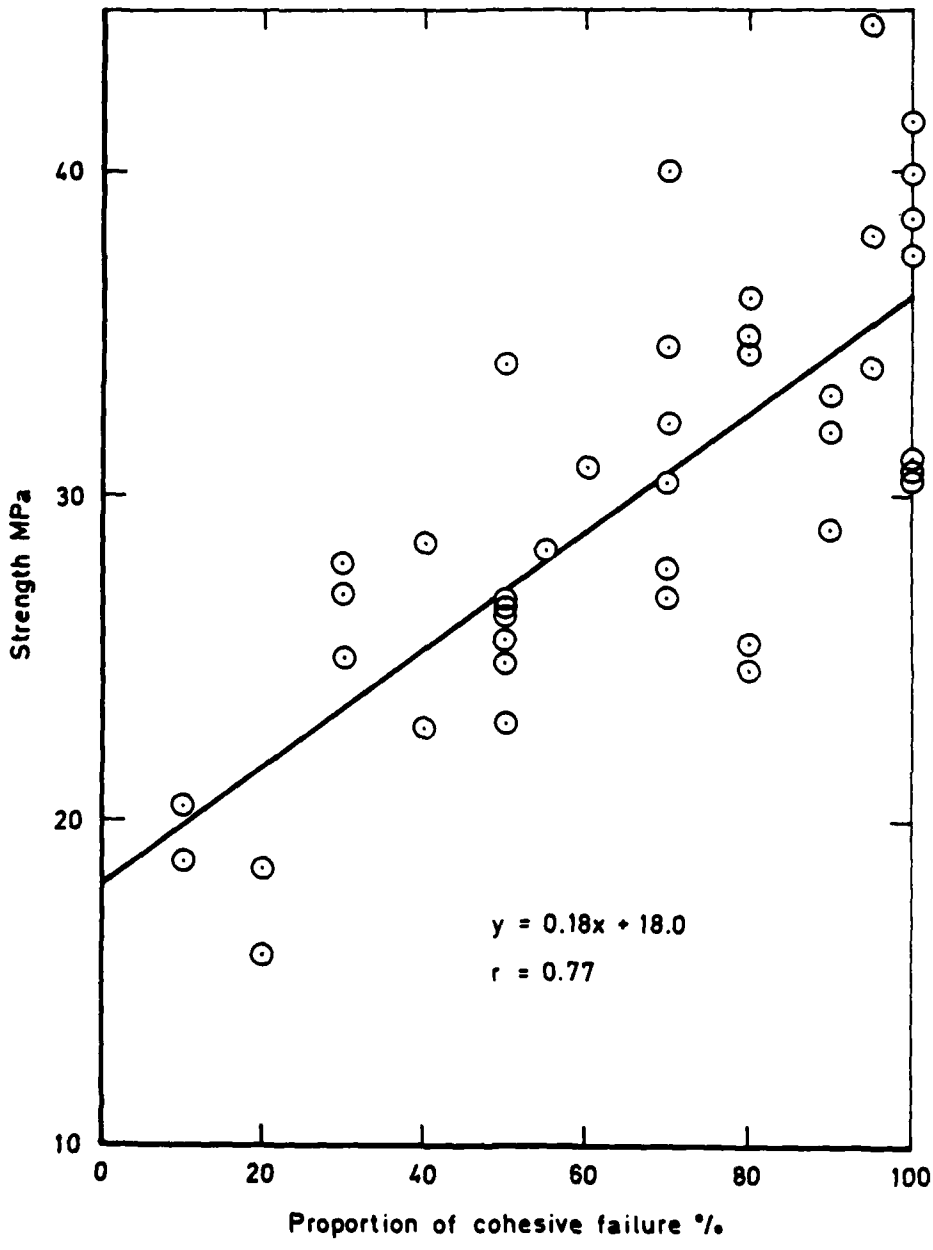

Fig 4 **Correlation of joint strength with proportion of cohesive failure (*ie* CA + CC) for metal-CFRP joints with adhesive M3**

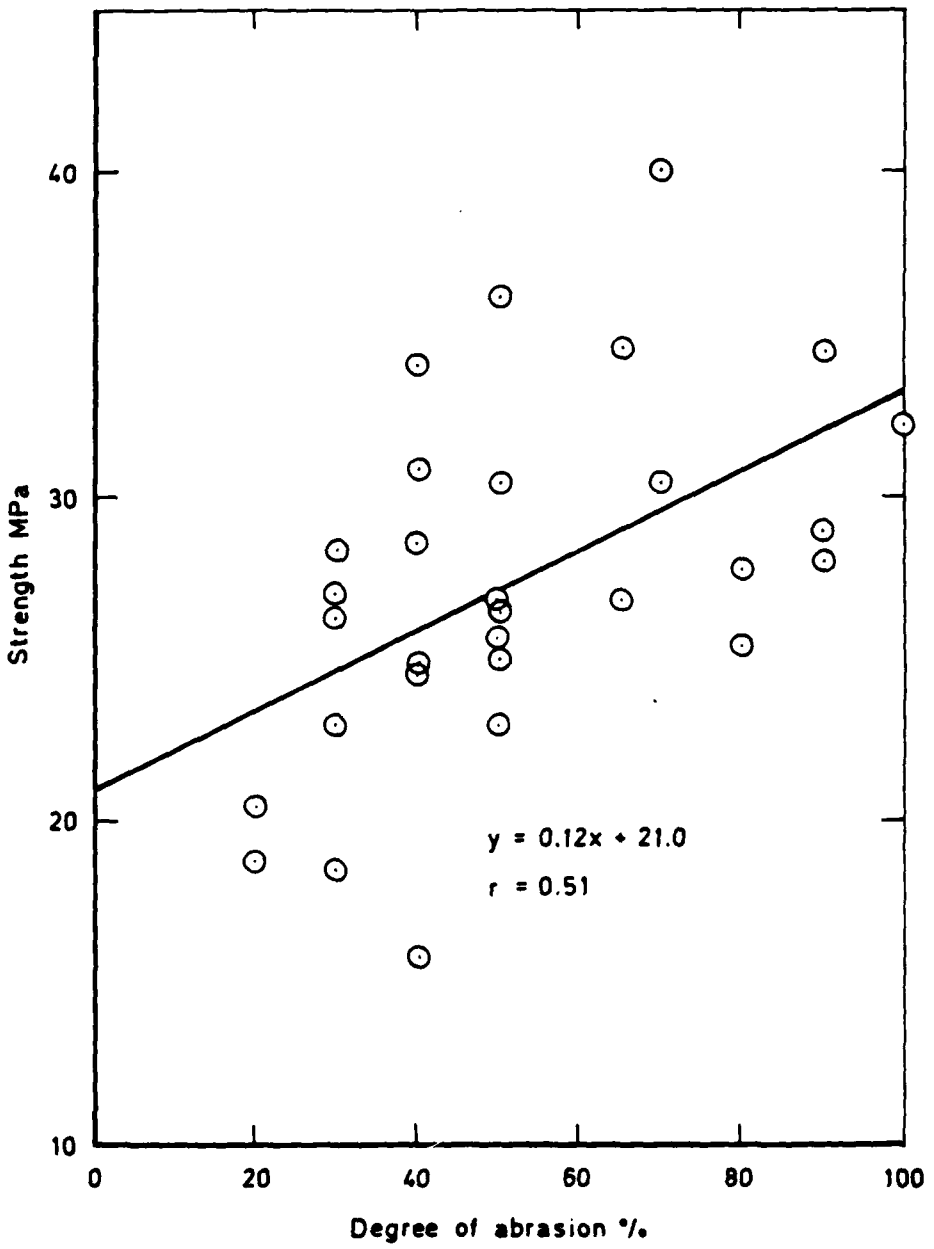

Fig 5 **Correlation of joint strength with degree of abrasion (*ie* proportion of composite surface covered by abrasion pits) for metal-CFRP joints with adhesive M3**

Fig 6

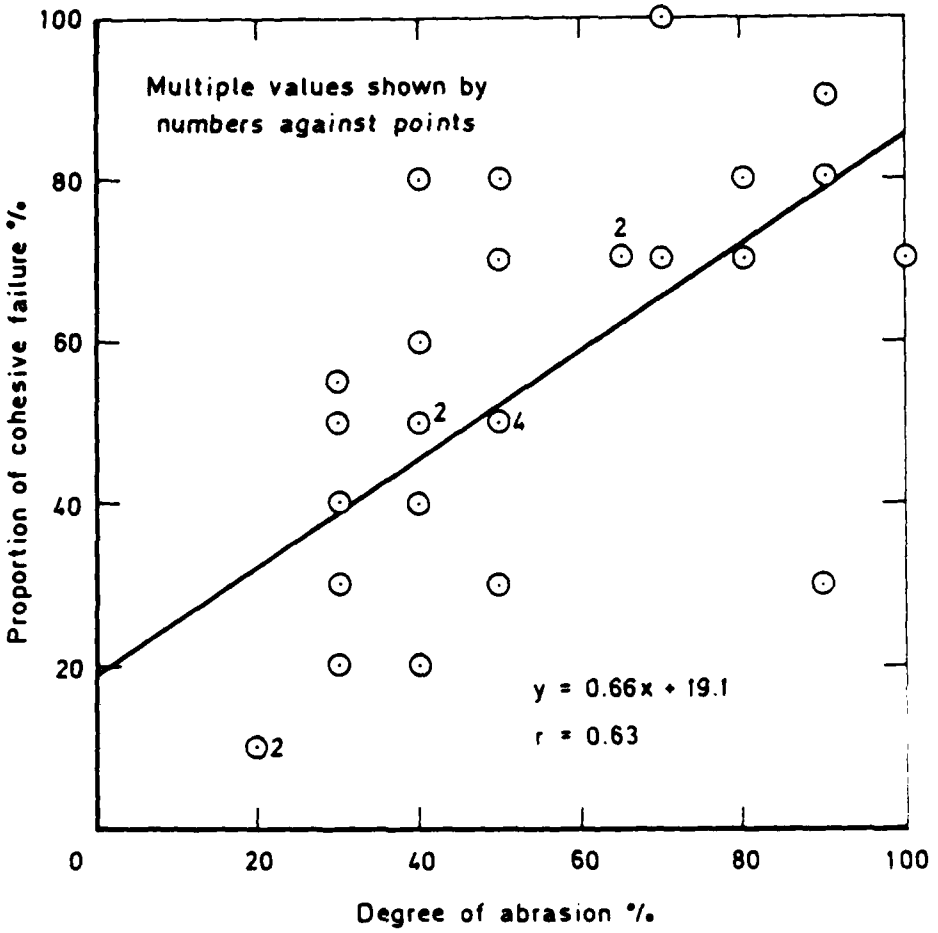

Fig 6 Correlation of proportion of cohesive failure with degree of abrasion for metal-CFRP joints with adhesive M3

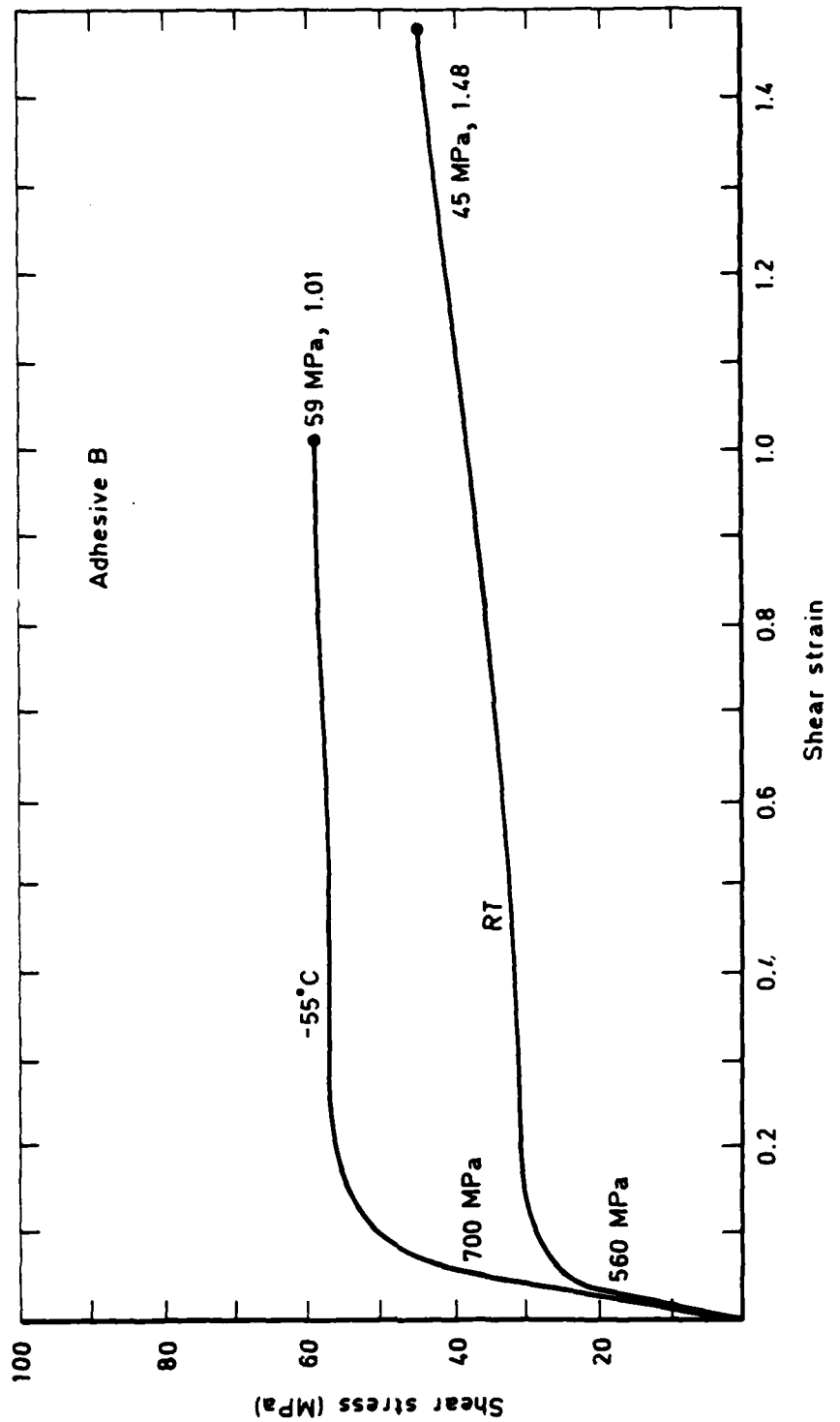

Fig 7 Thick adherend shear stress/strain curves for adhesive B at −55°C and ambient temperature (from Ref 10)

Fig 8

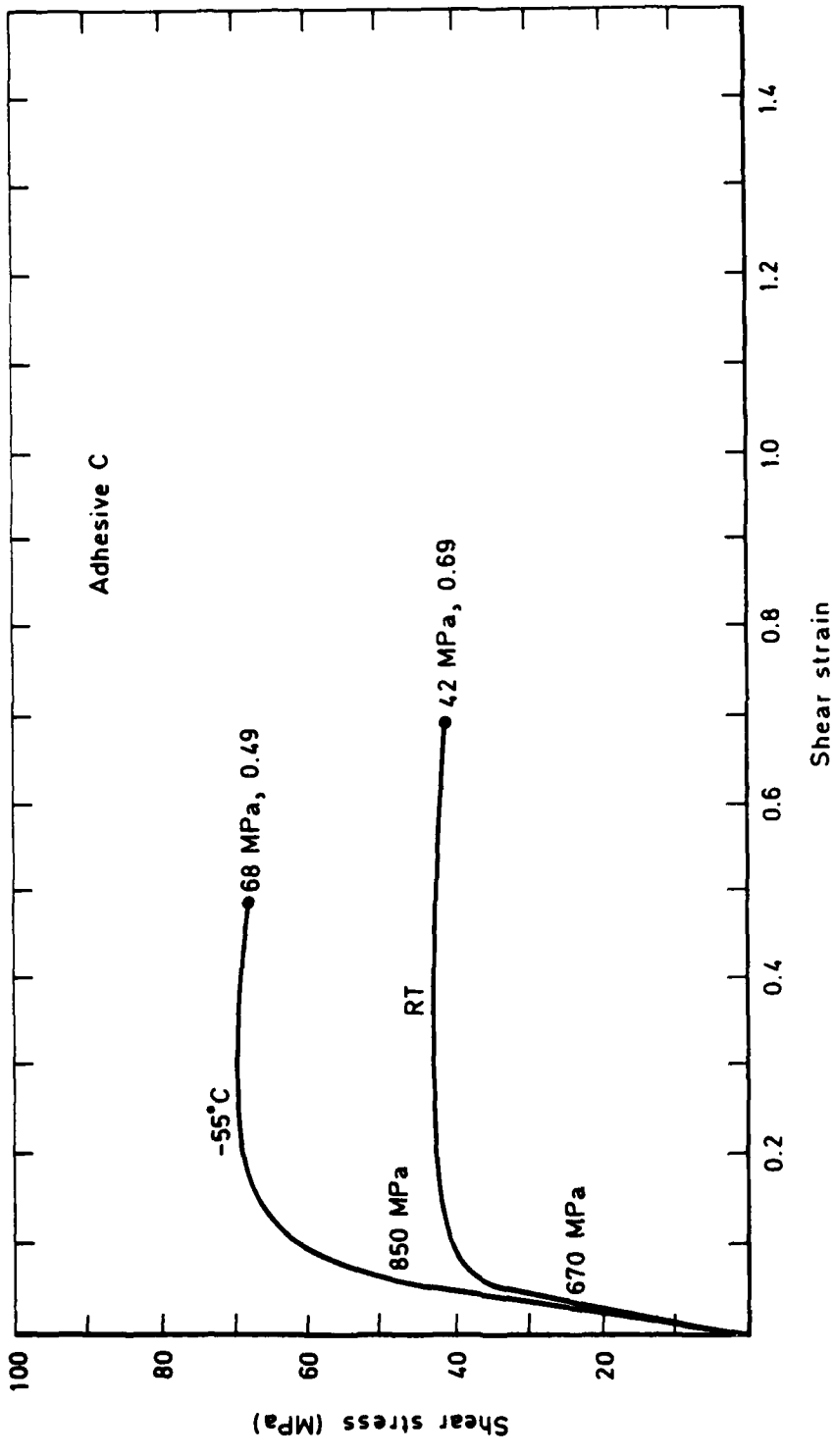

Fig 8 Thick adherend shear stress/strain curves for adhesive C at -55°C and ambient temperature (from Ref 10)

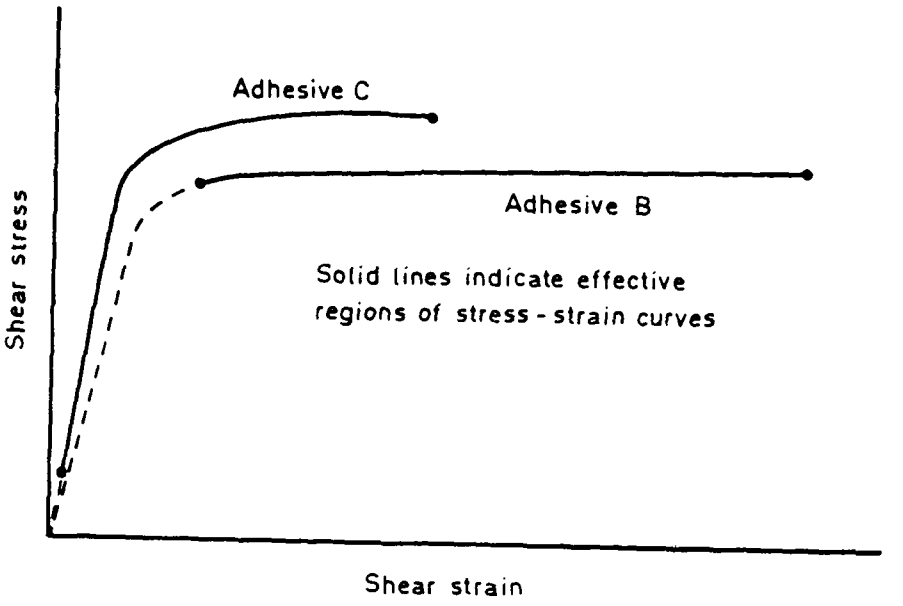

Fig 9a Hypothetical qualitative illustration of effective regions of shear stress-strain curves for adhesives B and C at point of failure in a metal-CFRP joint at −55°C

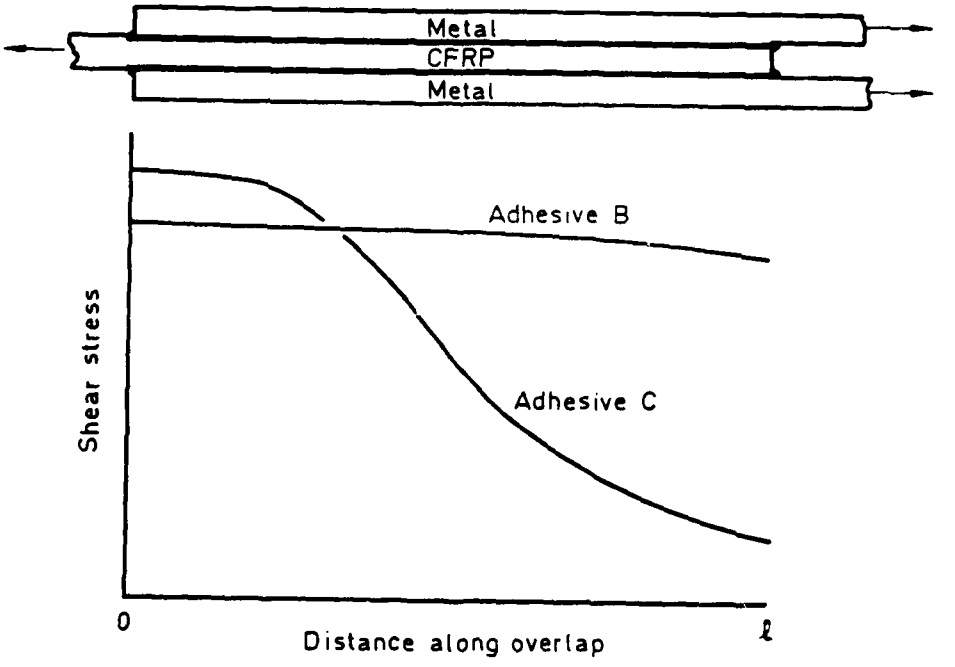

Fig 9b Hypothetical adhesive shear stress distribution along overlap length at point of failure in a metal-CFRP joint at −55°C, for adhesives B and C

REPORT DOCUMENTATION PAGE

Overall security classification of this page

UNCLASSIFIED

As far as possible this page should contain only unclassified information. If it is necessary to enter classified information, the box above must be marked to indicate the classification, e.g. Restricted, Confidential or Secret.

1. DRIC Reference (to be added by DRIC)	2. Originator's Reference	3. Agency Reference	4. Report Security Classification/Marking
	RAE TR 82102	N/A	UNLIMITED

5. DRIC Code for Originator	6. Originator (Corporate Author) Name and Location
7673000W	Royal Aircraft Establishment, Farnborough, Hants, UK
5a. Sponsoring Agency's Code	6a. Sponsoring Agency (Contract Authority) Name and Location
N/A	N/A

7. Title A comparison of the strengths of metal-metal and metal-CFRP adhesive bonded joints at various test temperatures

7a. (For Translations) Title in Foreign Language

7b. (For Conference Papers) Title, Place and Date of Conference

8. Author 1. Surname, Initials	9a. Author 2	9b. Authors 3, 4	10. Date	Pages	Refs.
Stone, M.H.			October 1982	39	26

11. Contract Number	12. Period	13. Project	14. Other Reference Nos.
N/A	N/A		Materials/ Structures 13

15. Distribution statement
(a) Controlled by –

(b) Special limitations (if any) –

16. Descriptors (Keywords) (Descriptors marked * are selected from TEST)
Acrylic resins*. Adhesive bonding*. Adhesive strength*. Aluminium alloys*. Bonded joints*. Epoxy resins*. Graphite composites*. Lap joints*. Shear strength*. Shear stress*. Thermal stresses*. Titanium alloys*.

17. Abstract

Tests on double lap joints bonded with a range of adhesives showed that differential thermal contraction of the adherends in metal-CFRP joints can greatly reduce strengths relative to metal-metal joints, particularly at low temperatures. However, the effect varied widely between adhesives, and relatively high strengths were obtained for an adhesive with a high strain to failure.

Strengths of metal-CFRP joints were much higher when titanium was substituted for aluminium, as expected from the lower expansion coefficient of titanium. However, attempts to reduce thermal stress by lowering the stress-free temperature with the use of reduced cure temperatures were unsuccessful, possibly because the adhesives did not develop their full toughness.

The low transverse tensile strength of CFRP also contributed in some cases to the reduced strength of metal-CFRP joints, relative to metal-metal joints.

F5910/1

RAE Form A143

outer metal adherend.

(e) Strength was correlated with proportion of AC failure (see section 4.2).

(f) Much of the CA failure was close to the CFRP surface, either at the primer/adhesive interface or within the primer layer: the former location predominated on the -55°C samples.